JOURNAL OF GUIDANCE, CONTROL, AND DYNAMICS
Vol. 30, No. 4, July–August 2007

Optimization of Multiple-Impulse, Multiple-Revolution, Rendezvous-Phasing Maneuvers

Ya-Zhong Luo,* Guo-Jin Tang,† Yong-Jun Lei,‡ and Hai-Yang Li§
National University of Defense Technology, 410073 Changsha, People's Republic of China

DOI: 10.2514/1.25620

A new hybrid optimization approach is proposed for the design of a rendezvous-phasing strategy with combined maneuvers, which is normally considered as a complex multiple-impulse, multiple-revolution, nonlinear rendezvous problem. In this approach, a feasible iteration optimization model is first formulated using a multiple-revolution Lambert algorithm, and a parallel simulated annealing algorithm is employed to locate the unperturbed solution. Subsequently, an infeasible iteration optimization model accounting for trajectory perturbations is formulated, and a sequential quadratic programming algorithm is used to obtain the perturbed solution, with the unperturbed solution as an initial reference solution. The global convergence ability of the proposed approach is verified by solving a classical same-circle rendezvous problem. Two different solutions satisfying Lawden's necessary optimality conditions are located and one solution outperforms an optimal solution previously reported. The proposed approach is further evaluated in a practical two-day rendezvous-phasing mission with different initial conditions. It is shown that this approach is effective and efficient and the combined maneuvers can save propellant at a range of 4–35% when compared with the special-point maneuvers.

I. Introduction

THE rendezvous and docking (RVD) mission can be divided into a number of major phases: launch, phasing, far-range rendezvous, close-range rendezvous, and docking. The objective of the phasing segment is to reduce the phase angle between the chaser and the target spacecraft, based on the fact that a lower orbit has a shorter orbital period [1]. During the rendezvous-phasing segment, launch injection errors on inclination and right ascension of the ascending node (RAAN) will be corrected successively. The phasing segment can take anywhere from one–three days (Mir/Progress, Shuttle/International Space Station) to two weeks (Zvezda–International Space Station) [1,2].

The design of a phasing strategy is an important part of the mission planning for most practical rendezvous missions. A well-designed phasing strategy not only saves propellant but improves safety. There are two widely used phasing strategies. One is the Soyuz/Progress phasing strategy [1–3], which is based on the impulsive maneuvers that combine in-plane and out-of-plane components. Labourdette and Baranov [2] and Baranov [3] proposed a semi-analytical method for this type of phasing strategy using a linearized dynamic model. The other phasing strategy (i.e., the strategy of the space shuttle), is based on impulsive maneuvers at special points (such as orbit apogee) for which desired orbit changes can be achieved using minimum propellant [1,4]. Recently, Luo et al. [5] reported an optimization approach for the phasing strategy using special-point maneuvers.

The rendezvous-phasing problem is a multiple-impulse, multiple-revolution nonlinear rendezvous problem. The widely used tools for solving the nonlinear impulsive rendezvous problem include primer vector theory [6] (based on the original work of Lawden [7]) and the Lambert algorithm [6,8]. By using these tools and the classical gradient-based optimization algorithms, Jezewski and Rozendaal [8], Gross and Prussing [9], Prussing and Chiu [10], and Hughes et al. [11] solved different types of multiple-impulse unperturbed two-body impulsive rendezvous problems. Prussing [12], Shen and Tsiotras [13] and Han and Xie [14] reported the analytical two-impulse multiple-revolution Lambert solution. In this paper, we provide a new approach for optimizing rendezvous-phasing combined maneuvers using the multiple-revolution Lambert algorithm and the recently developed optimization techniques. In addition, we also develop some techniques to obtain a perturbed solution that is different from [8–14], in which only an unperturbed two-body solution is obtained.

The approach adopted for solving the rendezvous-phasing problem is as follows. A parallel simulated annealing is first used to locate an unperturbed solution using an analytical two-body propagator and the multiple-revolution Lambert algorithm. This unperturbed solution is then used as an initial reference solution for the perturbed problem, and a sequential quadratic programming (SQP) algorithm is applied to locate an accurate solution using a high-fidelity trajectory model.

II. Rendezvous-Phasing Problem

In general, the impulse-based maneuver is adopted for phasing. The goal of phasing-strategy design is to design the impulse vectors, that is, to determine the optimal times and locations of the impulses. As a rule, all phasing maneuvers are controlled from the ground. Phasing ends with the acquisition of either an *initial aim point* or with the achievement of a set of margins for position and velocity values at a certain range, called the *trajectory gate* or *entry gate* [1]. Figure 1 depicts the initial and the final conditions for the rendezvous-phasing problem considered in this paper. The margins of the aim point (the gate) must be achieved to make the final part of the approach possible. The aim point or gate will be on the target orbit, or very close to it, and from this position, the far-range relative rendezvous operations can commence. In this paper, the aim point described in the target orbit frame is employed as the phasing final condition. The special-point maneuvers employ impulsive maneuvers, with only in-plane or out-of-plane components to adjust orbital phasing angle and correct orbital plane errors (inclination and RAAN). It has been shown that combining in-plane and out-of-plane components of maneuvers could save propellant [2]. This paper is mainly focused on developing a new approach for optimizing a phasing strategy with combined maneuvers.

Received 4 June 2006; revision received 6 January 2007; accepted for publication 8 January 2007.

*Ph.D. Candidate, College of Aerospace and Material Engineering; yzluo@sohu.com. Student Member AIAA (Corresponding Author).
†Professor, College of Aerospace and Material Engineering.
‡Professor, College of Aerospace and Material Engineering.
§Associate Professor, College of Aerospace and Material Engineering.

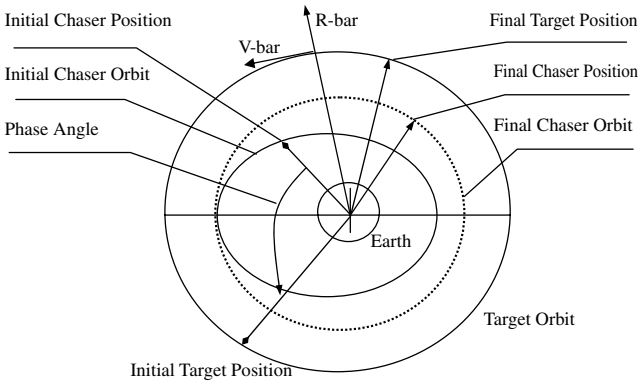

Fig. 1 Definition of phase angle and the initial and final conditions for rendezvous-phasing problem.

III. Multiple-Revolution Lambert Rendezvous Algorithm

A. Two-Impulse Lambert Rendezvous

The geometry for a two-impulse rendezvous is shown in Fig. 2. The initial position and velocity vectors of the chaser ($\boldsymbol{r}_1$ and $\boldsymbol{v}_{10}$), the targets $\boldsymbol{r}_{1\text{tar}}$ and $\boldsymbol{v}_{1\text{tar}}$, and the transfer time Δt are known. The final rendezvous conditions $\boldsymbol{X}_f$ are specified, which are always represented by the relative position and velocity vector between the chaser and the target. The solution to the initial and final velocity increments of the chaser ($\Delta\boldsymbol{v}_1$ and $\Delta\boldsymbol{v}_2$) is a standard Lambert's problem. The universal variables algorithm [15] is used to solve Lambert's problem.

B. Multiple-Revolution Lambert Rendezvous Algorithm

If Δt is small, there is only one transfer orbit. However, if Δt is relatively large, the transfer orbit obtained by the Lambert algorithm has a large eccentricity. This large-eccentricity orbit is not acceptable in practical engineering because of its huge propellant. Under this condition, it is necessary to find a transfer orbit in which the chaser first parks L (an integer number) revolutions and then rendezvouses with the target. Prussing [12], Shen and Tsiotras [13], and Han and Xie [14] reported the two-impulse multiple-revolution Lambert rendezvous solutions. In this paper, a new simple multiple-revolution Lambert rendezvous algorithm is provided by considering the practical background of the phasing rendezvous.

Assuming that the flight time from s_1 to s_2 is t_{tran}, Lambert's problem Lambert($\boldsymbol{r}_1, \boldsymbol{r}_2, t_{\text{tran}}$) is solved and the velocity vector of the parking obit $\boldsymbol{v}_1$ is obtained. The orbital period of the parking orbit T_p is calculated, whereas $\boldsymbol{r}_1$ and $\boldsymbol{v}_1$ are known. Thus, the critical step for solving the multiple-revolution, two-impulse rendezvous problem is to design t_{tran}. A simple iteration algorithm is employed to find t_{tran}, and the two-impulse multiple-revolution Lambert rendezvous algorithm is summarized as follows.

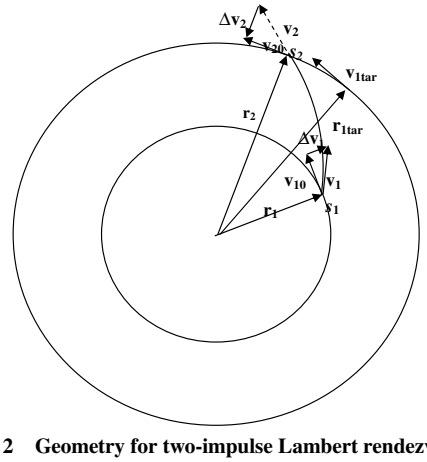

Fig. 2 Geometry for two-impulse Lambert rendezvous.

Step 1) Calculate the current orbital period T_0.

Step 2) If $\Delta t < T_0$, no parking orbit is required, solve Lambert's problem Lambert($\boldsymbol{r}_1, \boldsymbol{r}_2, \Delta t$), and get $\Delta\boldsymbol{v}_1$ and $\Delta\boldsymbol{v}_2$; otherwise, go to step 3.

Step 3) Solve $y(t_{\text{tran}}) = \Delta t - LT_p - t_{\text{tran}} = 0$ by Newton's method, and obtain the solution t^*_{tran}.

Step 4) Solve Lambert's problem Lambert($\boldsymbol{r}_1, \boldsymbol{r}_2, t^*_{\text{tran}}$), and get $\Delta\boldsymbol{v}_1$ and $\Delta\boldsymbol{v}_2$.

In this paper, only the low-Earth rendezvous-phasing problem is considered, and the phasing orbit should be between the chaser orbit and the target orbit so that the orbital period does not change much during the rendezvous-phasing segment. For this reason, we can define L as the maximum integer number less than $\Delta t/T_0$.

IV. Unperturbed Solution

A. Multi-Impulse Rendezvous Problem

The initial conditions for rendezvous are $\boldsymbol{r}_0$, $\boldsymbol{v}_0$, and t_0, and the terminal conditions are $\boldsymbol{r}_f$, $\boldsymbol{v}_f$, and t_f.

The dynamic equations are

$$\ddot{\boldsymbol{r}} = -\mu(\boldsymbol{r}/r^3) \tag{1}$$

Assuming that an impulsive $\Delta\boldsymbol{v}_i$ is applied (the superscript $-$ indicates the state before an impulse and the superscript $+$ indicates the state after an impulse), we get

$$\begin{cases} \boldsymbol{r}_i^+ = \boldsymbol{r}_i^- \\ t_i^+ = t_i^- \\ \Delta\boldsymbol{v}_i = \boldsymbol{v}_i^+ - \boldsymbol{v}_i^- \end{cases} \tag{2}$$

Without loss of generality, let

$$\boldsymbol{r}_i = \boldsymbol{r}_i^+ = \boldsymbol{r}_i^- \qquad t_i = t_i^+ = t_i^- \tag{3}$$

and assume that $\boldsymbol{r}(t+\Delta t) = \boldsymbol{f}[\boldsymbol{r}(t), \boldsymbol{v}(t), t, t+\Delta t]$ and $\boldsymbol{v}(t+\Delta t) = \boldsymbol{g}[\boldsymbol{r}(t), \mathbf{v}(t), t, t+\Delta t]$ are the solutions to Eqs. (1).

For an intermediate impulse $i \neq 1$, $i \neq n$, where $n(\geq 2)$ is the number of impulses, the following conditions must be satisfied:

$$\boldsymbol{r}_i = \boldsymbol{f}\left(\boldsymbol{r}_{i-1}, \boldsymbol{v}_{i-1}^+, t_{i-1}, t_i\right) \qquad \boldsymbol{v}_i^- = \boldsymbol{g}\left(\boldsymbol{r}_{i-1}, \boldsymbol{v}_{i-1}^+, t_{i-1}, t_i\right) \tag{4}$$

The constraints corresponding to the initial conditions are given by

$$\boldsymbol{r}_1 = \boldsymbol{f}(\boldsymbol{r}_0, \boldsymbol{v}_0, t_0, t_1) \qquad \boldsymbol{v}_1^- = \boldsymbol{g}(\boldsymbol{r}_0, \boldsymbol{v}_0, t_0, t_1) \tag{5}$$

where t_1 is the time of the first impulse.

A similar set of constraints applied at the final conditions are given by

$$\boldsymbol{r}_n = \boldsymbol{f}(\boldsymbol{r}_f, \boldsymbol{v}_f, t_f, t_n) \qquad \boldsymbol{v}_n^+ = \boldsymbol{g}(\boldsymbol{r}_f, \boldsymbol{v}_f, t_f, t_n) \tag{6}$$

In summary, the general fuel-optimal, multi-impulse rendezvous problem is to find $(\boldsymbol{r}_i, \boldsymbol{v}_i^+, \boldsymbol{v}_i^-, t_i)$, where $i = 1, 2, \cdots, n$, that satisfy the following constraints [11]:

$$\begin{cases} \boldsymbol{r}_1 = \boldsymbol{f}(\boldsymbol{r}_0, \boldsymbol{v}_0, t_0, t_1) \\ \boldsymbol{v}_1^- = \boldsymbol{g}(\boldsymbol{r}_0, \boldsymbol{v}_0, t_0, t_1) \\ \boldsymbol{r}_i = \boldsymbol{f}(\boldsymbol{r}_{i-1}, \boldsymbol{v}_{i-1}^+, t_{i-1}, t_i) \\ \boldsymbol{v}_i^- = \boldsymbol{g}(\boldsymbol{r}_{i-1}, \boldsymbol{v}_{i-1}^+, t_{i-1}, t_i) \\ \boldsymbol{r}_n = \boldsymbol{f}(\boldsymbol{r}_f, \boldsymbol{v}_f, t_f, t_n) \\ \boldsymbol{v}_n^+ = \boldsymbol{g}(\boldsymbol{r}_f, \boldsymbol{v}_f, t_f, t_n) \end{cases} \tag{7}$$

and to minimize the total velocity characteristic

$$J = \Delta v = \sum_{i=1}^{n} |\Delta\boldsymbol{v}_i| \tag{8}$$

B. Feasible Iteration Optimization Model

The parameter optimization methods to the optimization problem described by Eqs. (7) and (8) can be divided into two categories called the *feasible iteration approach* and the *infeasible iteration approach* [11]. In the feasible iteration approach, each evaluation of the objective function produces a feasible solution that implicitly satisfies the rendezvous conditions. The feasible iteration approach requires a careful choice of the independent variables, whereas in the infeasible iteration approach, there is less restriction on the choice of independent variables. In the infeasible iteration approach, the rendezvous conditions are not necessarily satisfied for each objective function evaluation. The rendezvous conditions are satisfied upon convergence of the numerical optimization algorithm. Thus, in the infeasible iteration approach, the constraints must be defined carefully, and the optimization algorithm must be able to handle nonlinear constraints. Hughes et al. [11] discussed details on how to formulate the optimization model of the feasible iteration approach. The applied optimization model of the feasible iteration approach is as follows.

The chosen independent variables (i.e., the optimization variables) are impulse times and the first $n-2$ impulse vectors:

$$t_i \qquad i=1,2,\cdots,n \qquad \Delta \boldsymbol{v}_j \qquad j=1,2,\cdots,n-2 \tag{9}$$

Calculating $\boldsymbol{r}_1$ and $\boldsymbol{v}_1^-$ in Eq. (5) and $\boldsymbol{r}_n$ and $\boldsymbol{v}_n^+$ in Eq. (6), we have

$$\begin{cases} \boldsymbol{v}_i^+ = \boldsymbol{v}_i^- + \Delta \boldsymbol{v}_i \\ \boldsymbol{r}_{i+1} = \boldsymbol{f}(\boldsymbol{r}_i, \boldsymbol{v}_i^+, t_i, t_{i+1}) \quad (i=1,2,\cdots,n-2) \\ \boldsymbol{v}_{i+1}^- = \boldsymbol{g}(\boldsymbol{r}_i, \boldsymbol{v}_i^+, t_i, t_{i+1}) \end{cases} \tag{10}$$

The rendezvous conditions are satisfied by solving Lambert's problem Lambert$(\boldsymbol{r}_{n-1}, \boldsymbol{r}_n, t_n - t_{n-1})$. With the solution for Lambert's problem, we can solve for $\Delta \boldsymbol{v}_{n-1}$ and $\Delta \boldsymbol{v}_n$ and we then solve Eq. (8) for the total Δv. For the phasing rendezvous, the last two impulses are always imposed on different revolutions and so the multiple-revolution Lambert algorithm is required.

For the multiple-revolution, multiple-impulse, rendezvous-phasing problem, it is more convenient to replace t_i with the number of revolutions N_i and the argument of latitude Φ_i in formulating the optimization model. In this study, N_i are not chosen as optimization variables. They are set in advance to satisfy the operational constraints such as orbit-determination requirements and communication-window constraints. Therefore, the final chosen optimization variables are

$$\Phi_i \qquad i=1,2,\cdots,n \qquad \Delta \boldsymbol{v}_j \qquad j=1,2,\cdots,n-2 \tag{11}$$

C. Optimization Technique: Parallel Simulated Annealing Using Simplex Method

The optimization of phasing maneuvers is very difficult due to the very long duration dedicated to rendezvous (several tens of vehicle revolutions). Although it can be formulated as an unconstrained problem using the multiple-revolution Lambert algorithm, the classical nonlinear optimization algorithms such as the SQP and Powell's algorithm have very poor performance in solving this problem, which was observed in our mathematical experiments. It is therefore highly desirable and necessary to introduce other new global optimization algorithms to solve this problem. The parallel simulated annealing using the simplex method (PSASM) is a recently developed new global optimization algorithm [16,17]. The PSASM combines the advantages of simulated annealing (SA) with that of the simplex method, and its flowchart is provided in the Appendix. It has been demonstrated that the PSASM algorithm has better global convergence ability and higher convergence rate than the SA, genetic algorithms (GAs), and some other evolutionary algorithms in functional and structural optimization [16] and low-thrust trajectory design [17]. In this paper, the PSASM is employed as a global optimizer for the unperturbed rendezvous-phasing problem.

V. Perturbed Solution

The solution obtained by the PSASM is an unperturbed solution. Using the unperturbed solution as the initial guess, the SQP is employed to obtain the perturbed solution.

A. General Dynamic Equations

The general dynamic equations for describing a spacecraft with all perturbations are known as Cowell's formulation [15]:

$$\begin{cases} \frac{\mathrm{d}\boldsymbol{v}}{\mathrm{d}t} = -\frac{\mu}{r^3}\boldsymbol{r} + \boldsymbol{a}_{\text{nonspherical}} + \boldsymbol{a}_{\text{drag}} + \boldsymbol{a}_{3-\text{body}} + \boldsymbol{a}_{\text{SR}} + \boldsymbol{a}_{\text{thrust}} + \boldsymbol{a}_{\text{other}} \\ \frac{\mathrm{d}\boldsymbol{r}}{\mathrm{d}t} = \boldsymbol{v} \end{cases} \tag{12}$$

where $\boldsymbol{r}$ and $\boldsymbol{v}$ are the position and velocity vectors, respectively; $\boldsymbol{a}_{\text{nonspherical}}$ is the perturbation acceleration caused by the nonspherical portion of the mass distribution of the central body; $\boldsymbol{a}_{\text{drag}}$ is the atmospheric drag perturbation acceleration; $\boldsymbol{a}_{3-\text{body}}$ is the third-body perturbation acceleration including the sun's and the moon's gravity; $\boldsymbol{a}_{\text{SR}}$ is the solar-radiation pressure perturbation acceleration; $\boldsymbol{a}_{\text{thrust}}$ is the thrust acceleration; and $\boldsymbol{a}_{\text{other}}$ is the perturbation acceleration caused by many other forces including tides. More details of these perturbations can be found in Vallado [15].

Through Eqs. (10) and (12), a multiple-impulse rendezvous problem can be solved with an accurate solution by numerically integrating both the chaser and target orbits. In this study, the classical orbit elements $\boldsymbol{E} = (a, i, e, \Omega, \omega, \nu)$ are employed to describe the rendezvous-phasing problem, where a is the semimajor axis, i is the inclination, e is the eccentricity, Ω is the right ascension of the ascending node (RAAN), ω is the argument of perigee, and ν is the true anomaly.

Among all the aforementioned perturbation forces, the J_2 effects are often dominant. For the perturbed problem, Vallado [15] proposed a simplified analytical propagation technique that captures the secular perturbative effects resulting from J_2. In this study, both the analytical J_2-perturbed propagator and the numerical integration method are applied. An eighth-order Runge–Kutta method [18] is used, and the integration step is 30 s.

B. Infeasible Iteration Optimization Model

It is convenient to describe a rendezvous problem using the relative state of the chaser with respect to the target. Herein, a relative coordinate (as shown in Fig. 3) is applied. Using the orbit coordinate, the relative state is denoted by $\boldsymbol{x} = (x, y, z, \dot{x}, \dot{y}, \dot{z})$.

The optimization variable vector $\boldsymbol{y}$ is

$$\boldsymbol{y} = (\Phi_i, \Delta \boldsymbol{v}_i) \qquad i=1,2,\cdots,n \tag{13}$$

The objective function is to minimize the total characteristic velocities:

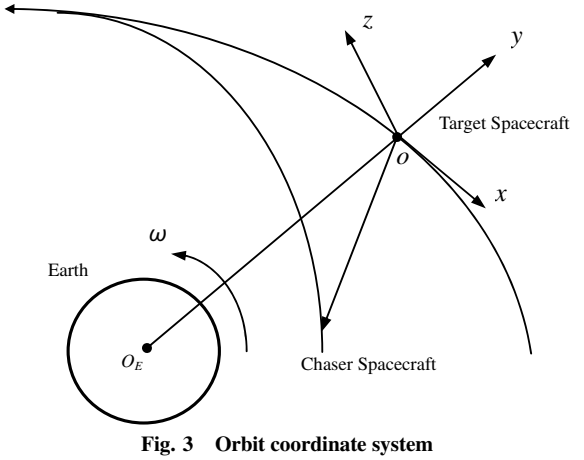

Fig. 3 Orbit coordinate system

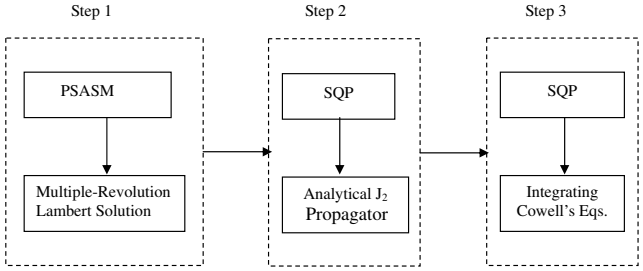

Fig. 4 Solution framework for optimizing rendezvous-phasing maneuvers.

$$J = \sum_{i=1}^{n} |\Delta \boldsymbol{v}_i| \tag{14}$$

The initial conditions at time t_0 are defined by

$$\boldsymbol{x}(t_0) - \boldsymbol{x}_0 = 0 \tag{15}$$

The terminal constraints at the final time t_f are defined by

$$\boldsymbol{x}(t_f) - \boldsymbol{x}_f = 0 \tag{16}$$

where $\boldsymbol{x}(t_f)$ is evaluated by numerically propagating both the target and the chaser orbits.

C. Optimization Technique: SQP

Equations (13–16) form an infeasible iteration optimization model for the fuel-optimal, multiple-impulse rendezvous problem. Because the model of the perturbed problem has only a little error from that of the unperturbed problem, it can be efficiently solved using the nonlinear programming solver with the unperturbed solution as the initial guess. The most widely used constrained optimization algorithm, SQP is employed to locate the perturbed solution.

The solution obtained by the PSASM is a two-body solution. To increase the convergence rate and robustness, the two-body solution is firstly modified by the SQP using an analytical J_2-perturbed propagator. Subsequently, the SQP is again employed to obtain the perturbed solution by numerically integrating the high-fidelity dynamic equations with the J_2-perturbed solution as the initial guess.

VI. Solution Framework

To summarize, the optimization approach proposed in this paper is a three-step cascade strategy, as described in Fig. 4.

In step 1, the PSASM is used to solve the optimization problem formulated in Eqs. (8–11). The multiple-revolution Lambert algorithm is employed to satisfy the rendezvous conditions naturally, and the analytical two-body propagator is used to calculate both the target and the chaser orbits. The unperturbed two-body solution is obtained by the PSASM.

In step 2, using the unperturbed solution obtained by the PSASM as the initial guess, the SQP is applied to solve the optimization problem formulated as Eqs. (13–16). The analytical J_2-perturbed propagator is used to calculate both the target and the chaser orbits. The J_2-perturbed solution is obtained by the SQP.

In step 3, using the J_2-perturbed solution as the initial guess, SQP is again employed to solve the optimization problem formulated as Eqs. (13–16) through numerically integrating Cowell's equations. In this study, the perturbations (including atmosphere drag and J_2, J_3, and J_4) are considered.

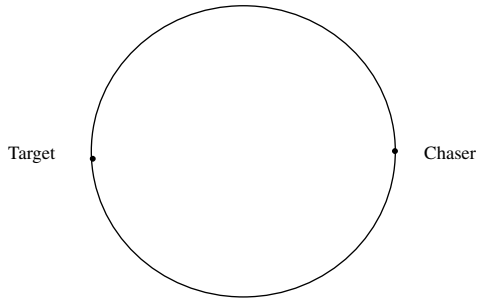

Fig. 5 Chaser and target in the same circular orbit.

VII. Analytical Problem Verification

First, we test the proposed approach by solving a classical problem: a same-circle rendezvous problem of a chaser in a circular orbit with a target in that same circular orbit [10,12]. A chaser and its target are shown in Fig. 5 for an initial separation angle of 180 deg. When the rendezvous transfer time is 2.3 times the orbital period, Prussing and Chiu [10] and Prussing [12] reported that an optimal four-impulse solution existed for this transfer time. Herein, a 400-km circular-orbit case is tested by the proposed approach. For convenient comparison, only the unperturbed two-body solution is obtained.

To our surprise, two different solutions are located by the PSASM. They are listed in Table 1. Figure 6 shows the primer vector magnitude histories corresponding to these two solutions. The transfer time is plotted in units of the circular-orbit period in Fig. 6. Clearly, these two solutions both satisfy all the necessary conditions for an optimal impulsive trajectory [12]. In units of the circular-orbit speed, the Δv of the second solution is calculated as 0.189, which is same as that provided by Prussing and Chiu [10]. Judging from the prime vector magnitude history, the second solution is that reported by Prussing and Chiu [10] and Prussing [12]. In a seminal paper, Jezewski and Rozendaal [8] pointed out that multiple solutions satisfying the classical necessary optimality conditions may exist for the nonlinear two-body impulsive rendezvous trajectory. The same-circle rendezvous problem has this peculiarity, which is also true for other cases, for example, 350- and 450-km circular orbit. In terms of the Δv cost, the first solution outperforms the second one by reducing the Δv cost by 13.4%. This solution was also reported by Colasurdo and Pastrone [19] and Sandrik [20].

Note that although the exact solution is symmetric about the midtime of the transfer (see Fig. 6, where $\Delta v_1 = \Delta v_4$, $\Delta v_2 = \Delta v_3$, and $t_4 - t_3 = t_2 - t_1$), small numerical discrepancies appear in Table 1.

VIII. Examples

In this section, we further test the proposed approach by a practical two-day rendezvous-phasing mission. The nominal initial conditions are

$$\boldsymbol{E}_{\text{tar}} = (6720.140\,\text{km}, 42\,\text{deg}, 0, 169.286\,\text{deg}, 0, 245\,\text{deg})$$

$$\boldsymbol{E}_{\text{cha}} = (6638.140\,\text{km}, 42.2\,\text{deg}, 0.009039, 169.686\,\text{deg}, 120\,\text{deg}, 1\,\text{deg})$$

Table 1 Two solutions for the 400-km same-circle rendezvous problem

	Impulses t_i(s) and Δv_i, m/s				
Index	$i = 1$	$i = 2$	$i = 3$	$i = 4$	Δv, m/s
1	$t_1 = 0$	$t_2 = 2648.9$	$t_3 = 10,130.1$	$t_4 = 12,773.3$	1256.3
	$\Delta v_1 = 391.6$	$\Delta v_2 = 236.5$	$\Delta v_3 = 235.8$	$\Delta v_4 = 392.5$	
2	$t_1 = 0$	$t_2 = 4414.6$	$t_3 = 8367.4$	$t_4 = 12,773.3$	1450.4
	$\Delta v_1 = 532.5$	$\Delta v_2 = 192.7$	$\Delta v_3 = 190.7$	$\Delta v_4 = 534.5$	

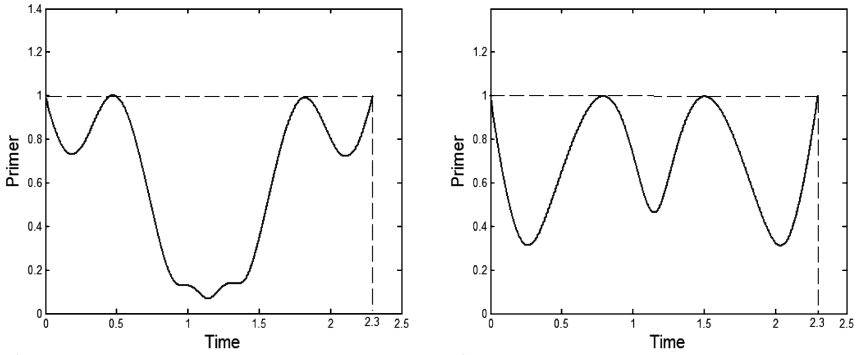

a) First solution **b) Second solution**

Fig. 6 Primer magnitude history for the optimal four-impulse trajectory.

The terminal conditions are

$$t_f = 140,000 \text{ s}$$

$$\boldsymbol{x}_f = (81.7, \ -29.3, \text{ and } 0.003 \text{ km}; \ -50.78, \ -0.02, \text{ and } -0.16 \text{ m/s})$$

The initial and terminal conditions are depicted in Fig. 1.

Let $\Delta\Omega = \Omega_{\text{cha}} - \Omega_{\text{tar}}$ denote the error of RAAN between the target and the chaser orbit and $\Delta i = i_{\text{cha}} - i_{\text{tar}}$ denote the error of inclination. The initial chaser orbit is always with a little dispersion to its nominal orbit because of the launch vehicle's guidance error. The plane errors, including the errors of RAAN and inclination, are the main contributions to the propellant of phasing maneuvers. Thus, it is necessary to analyze the influence of the plane errors on the phasing maneuvers. In our study, this phasing rendezvous problem is configured with different $\Delta\Omega$ and Δi:

1) For $\Delta i = 0.2$ deg, select 11 points of $\Delta\Omega$ at equal interval in the range of -1 to 1 deg.

2) For $\Delta\Omega = 0.4$ deg, select 11 points of Δi at equal interval in the range of -1 to 1 deg.

For each case, both the proposed approach and the special-point maneuvers approach [5] are tested. For the convenience of comparison, the total number of maneuvers is four, which are imposed on 6, 14, 17, and 22 revolutions, respectively, and are the same used by [5]. The search space of the design variables is presented in Table 2.

The relations between Δv vs $\Delta\Omega$ and Δv vs Δi are shown in Figs. 7 and 8, respectively. Figures 7 and 8 report the perturbed solution. The solutions of four test cases are provided in Table 3. Table 4 provides the impulses for the test case in which the unperturbed two-body and the perturbed solutions are reported ($\Delta i = 0.2$ deg and $\Delta\Omega = 0.4$ deg, respectively). The time cost for obtaining the perturbed solution is about 5 min on a Dell Dimension 8300 computer (CPU 2.8 GHz).

The statistical results of the PSASM, a continuous SA [16], and a floating-coded genetic algorithm (GA) [16] for the unperturbed solution with $\Delta i = 0.2$ deg and $\Delta\Omega = 0.4$ deg in 20 independent runs are listed in Table 5. All three algorithms end with a maximum number of function evaluations of 40,000.

From Tables 3–5 and Figs. 7 and 8, we can conclude the following:

1) The trends between Δv vs $\Delta\Omega$, and Δv vs Δi obtained by the proposed approach are similar to that of the special-point approach, showing the success of our proposed approach in obtaining a good solution for all test cases.

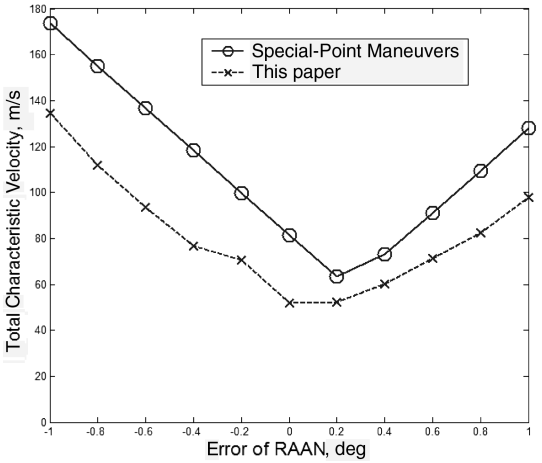

Fig. 7 Δv vs $\Delta\Omega$ ($\Delta i = 0.2$ deg).

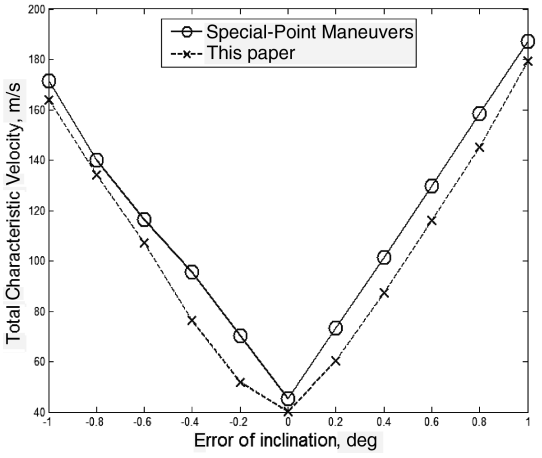

Fig. 8 Δv vs Δi ($\Delta\Omega = 0.4$ deg).

2) The combined maneuvers can significantly reduce Δv, compared with the special-point maneuvers. When $\Delta i = 0.2$ deg and $\Delta\Omega$ varies in the range of -1 to 1 deg, the reduction is from about 18 to 35%. When $\Delta\Omega = 0.4$ deg and Δi varies in the range of -1 to 1 deg, the reduction is from about 4 to 19%. For the same amount of $\Delta\Omega$ and Δi, the reduction of the former is much larger than the latter.

Table 2 Search space of the design variables

	Φ_i, deg				Δv_{Ii}, Δv_{Ji}, and Δv_{Ki}, m/s ($i = 1$, 2, 3, and 4)
Variables	$i = 1$	$i = 2$	$i = 3$	$i = 4$	
Search space	[290, 320]	[290, 360]	[40, 130]	[300, 330]	[−60, 60]

Table 3 The total characteristic velocity (Δv, m/s) for four cases obtained by the proposed approach and the special-point approach

Approach		Δi and $\Delta\Omega$			
		$\Delta i = 0.2$ deg	$\Delta i = 0.2$ deg	$\Delta i = -0.2$ deg	$\Delta i = -0.2$ deg
		$\Delta\Omega = 0.4$ deg	$\Delta\Omega = -0.4$ deg	$\Delta\Omega = 0.4$ deg	$\Delta\Omega = -0.4$ deg
Special-point approach	Unperturbed	98.51	98.57	98.35	98.08
	Perturbed	73.22	118.40	70.39	121.23
This paper	Unperturbed	74.82	58.57	57.58	78.93
	Perturbed	60.19	76.66	51.92	93.78

Table 4 Impulses corresponding with the first test case listed in Table 3

Approach		Impulses t_i(s) and Δv_i, m/s				Δv, m/s
		$i = 1$	$i = 2$	$i = 3$	$i = 4$	
Special-point approach	Unperturbed	$t_1 = 29,559.0$ $\Delta v_1 = 11.7$	$t_2 = 73,722.8$ $\Delta v_2 = 27.0$	$t_3 = 85,914.4$ $\Delta v_3 = 36.3$	$t_4 = 116,096.7$ $\Delta v_4 = 23.4$	98.5
	Perturbed	$t_1 = 29,606.7$ $\Delta v_1 = 13.3$	$t_2 = 73,661.0$ $\Delta v_2 = 26.5$	$t_3 = 85,835.9$ $\Delta v_3 = 14.4$	$t_4 = 116,180.9$ $\Delta v_4 = 19.0$	73.2
This paper	Unperturbed	$t_1 = 29,527.9$ $\Delta v_1 = 12.6$	$t_2 = 73,617.7$ $\Delta v_2 = 0.0$	$t_3 = 85,193.2$ $\Delta v_3 = 43.4$	$t_4 = 116,126.2$ $\Delta v_4 = 18.8$	74.8
	Perturbed	$t_1 = 29,487.1$ $\Delta v_1 = 8.6$	$t_2 = 73,459.3$ $\Delta v_2 = 17.8$	$t_3 = 85,022.6$ $\Delta v_3 = 19.8$	$t_4 = 115,994.5$ $\Delta v_4 = 14.0$	60.2

Table 5 Statistical results of different algorithms for unperturbed solution ($\Delta i = 0.2$ deg and $\Delta\Omega = 0.4$ deg)

Algorithms	Total characteristic velocity, Δv, m/s			
	Best	Worst	Mean	Std
PSASM	74.05	82.76	76.82	2.33
SA	73.16	109.32	81.65	8.10
GA	75.60	95.28	84.29	6.54

3) From Table 4, it is clear that the PSASM has better global convergence ability than the GA and the SA. Although the PSASM does not always locate the best solution in 20 runs, the Δv of the perturbed solution obtained by the SQP is always about 61–62 m/s. The PSASM is effective at locating an initial global reference solution to the perturbed solution, which guarantees the global convergence ability of the proposed approach.

It is not our purpose to show that the phasing strategy with combined maneuvers is better than the phasing strategy with special-point maneuvers; instead, our study shows that the combined maneuvers can save propellant. When designing an operational rendezvous-phasing mission, in addition to the propellant, other performances should also be considered, such as tolerance to failure, execution simplicity of maneuvers, etc. Our experiment showed that the phasing strategy with combined maneuvers can be well suited to different phasing schemes. If we change the revolutions of the maneuvers, as shown in Table 6, it is found that the Δv vary little.

IX. Conclusions

A new approach using the multiple-revolution Lambert algorithm, a parallel simulated annealing algorithm and sequential quadratic programming is proposed for optimizing a rendezvous-phasing strategy with combined maneuvers. The proposed approach locates a solution better than a reported optimal solution for the classical same-circle rendezvous problem. A practical two-day rendezvous-phasing mission with different configurations is also examined using our proposed approach. The results of a large number of experiments show that the proposed approach is quick and robust in locating the global solution. Compared with the special-point maneuvers, it has been proven that the combined maneuver can save propellant.

Table 6 Δv (m/s) for different phasing schemes ($\Delta i = 0.2$ deg and $\Delta\Omega = 0.4$ deg, perturbed)

Index	N_i ($i = 1, 2, 3, 4$)	Δv, m/s
1	6, 14, 17, 22	60.2
2	5, 15, 20, 26	61.0
3	6, 10, 23, 26	60.3

Appendix: Parallel Simulated Annealing Using the Simplex Method

The optimization procedure of PSASM is described in Fig. A1. This procedure is explained as follows.

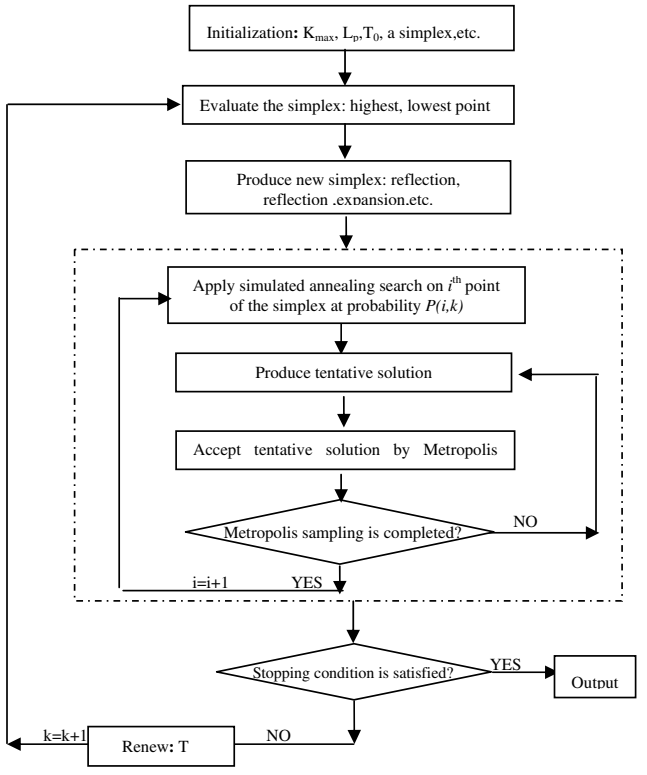

Fig. A1 Optimization procedure of parallel simulated annealing using the simplex method.

Step 1) A simplex (including the $n+1$ design vector) and other parameters (such as the initial temperature T_0 and the length of the Metropolis sampling L_p) are initialized, $k=1$.

Step 2) The simplex is evaluated and the highest, second-highest, and lowest points are determined.

Step 3) A new simplex is produced by reflection, reflection and expansion, etc.

Step 4) Simulated annealing search is applied on the ith point of the simplex (to be referred to as x^i) at probability $P(i,k)[P(i,k)=\exp(-k/k_{\max})]$, $i=1,2,\ldots,n_0$.

Step 4.1) Make the initial solution for the Metropolis sampling at the current temperature T_k:$y_l^i=x^i$, $l=1$.

Step 4.2) Produce the tentative solution y_{l+1}^i using the neighbor search function.

Step 4.3) Replace y_l^i with y_{l+1}^i using the Metropolis rule $l+=1$.

Step 4.4) If $l>L_{p,}$ $x^i=y_l^i$, go to step 5; otherwise, go to step 4.1.

Step 5) The PSASM is terminated if $k>k_{\max}$; otherwise, $k=k+1$, T_k is renewed, go to step 2.

Acknowledgments

The paper is supported by the China Postdoctoral Science Foundation (ref. 20060390892), the Science Project of the National University of Defense Technology (ref. JC06-01-01), and the Ph.D. Programs Foundation of the Ministry of Education of China (ref. 20069998002). The authors thank the Associate Editor and the reviewers for their suggestions to improve this paper.

References

[1] Fehse, W., *Automated Rendezvous and Docking of Spacecraft*, Cambridge Univ. Press, London, 2003, pp. 12–13, 441–449.

[2] Labourdette, P., and Baranov, A. A., "Strategies for On-Orbit Rendezvous Circling Mars," *Advances in the Astronautical Sciences*, Vol. 109, 2002, pp. 1351–1368.

[3] Baranov, A. A., "An Algorithm for Calculating Parameters of Multi-Orbit Maneuvers in Remote Guidance," *Cosmic Research*, Vol. 28, No. 1, 1990, pp. 61–67 (translation of *Kosmicheskie Issledovaniya*).

[4] *Shuttle Press Kit: STS-92* [online press kit], http://www.shuttlepresskit.com/STS-92/, [retrieved 25 Mar. 2007].

[5] Luo, Y. Z., Li, H. Y., Tang, G. J., "Hybrid Approach to Optimize a Rendezvous Phasing Strategy," *Journal of Guidance, Control, and Dynamics*, Vol. 30, No. 1, 2006, pp. 185–191.

[6] Lion, P. M., and Handelsman, M., "Primer Vector on Fixed-Time Impulsive Trajectories," *AIAA Journal*, Vol. 6, No. 1, 1968, pp. 127–132.

[7] Lawden, D. F., *Optimal Trajectories for Space Navigation*, Butterworths, London, 1963.

[8] Jezewski, D. J., and Rozendaal, H. L., "An Efficient Method for Calculating Optimal Free-Space N-Impulse Trajectories," *AIAA Journal*, Vol. 6, No. 11, 1968, pp. 2160–2165.

[9] Gross, L. R., and Prussing, J. E., "Optimal Multiple-Impulse Direct Ascent Fixed-Time Rendezvous," *AIAA Journal*, Vol. 12, No. 7, 1974, pp. 885–889.

[10] Prussing, J. E., and Chiu, J. H., "Optimal Multiple-Impulse Time-Fixed Rendezvous Between Circular Orbits," *Journal of Guidance, Control, and Dynamics*, Vol. 9, No. 1, 1986, pp. 17–22.

[11] Hughes, S. P., Mailhe, L. M., and Guzman, J. J., "A Comparison of Trajectory Optimization Methods for the Impulsive Minimum Fuel Rendezvous Problem," *Advances in the Astronautical Sciences*, Vol. 113, 2003, pp. 85–104.

[12] Prussing, J. E., "A Class of Optimal Two-Impulse Rendezvous Using Multiple-Revolution Lambert Solutions," *Journal of the Astronautical Sciences*, Vol. 48, No. 2, 2000, pp. 31–148.

[13] Shen, H. J., and Tsiotras, P., "Optimal Two-Impulse Rendezvous Using Multiple-Revolution Lambert Solutions," *Journal of Guidance, Control, and Dynamics*, Vol. 26, No. 1, 2003, pp. 50–61.

[14] Han, C., and Xie, H. W., "Study on the Multi-Revolution Lambert Transfer Algorithm for Rendezvous," *Chinese Space Science and Technology*, Vol. 24, No. 5, 2004, pp. 9–13.

[15] Vallado, D. A., *Fundamentals of Astrodynamics and Applications*, 2nd ed., Microscosm Press, 2001, El Segundo, CA, pp. 462–464, 497–502.

[16] Luo, Y. Z., and Tang, G. J., "Parallel Simulated Annealing Using Simplex Method," *AIAA Journal*, Vol. 44, No. 12, 2006, pp. 3143–3146; also AIAA Paper 2004-4584, 2004.

[17] Luo, Y. Z., and Tang, G. J., "Near-Optimal Low-Thrust Orbit Transfer Generated by Parallel Simulated Annealing," International Astronautical Congress, Paper 04-A.6.10, 2004.

[18] Fehlberg, E., "Classical Fifth-, Sixth-, Seventh-, and Eighth-Order Runge–Kutta Formulation with Stepsize Control," NASA TR-R-287, 1968.

[19] Colasurdo, G., and Pastrone, D., "Indirect Optimization Method for Impulsive Transfers," *A Collection of Technical Papers: AIAA/AAS Astrodynamics Conference*, CP9411, 1994, pp. 441–448; also AIAA Paper 1994-3762.

[20] Sandrik, S. L., "Primer-Optimized Results and Trends for Circular Phasing and Other Circle-to-Circle Impulsive Coplanar Rendezvous," Ph.D. Thesis, Dept. of Aerospace Engineering, Univ. of Illinois at Urbana-Champaign, Urbana, IL, 2006.